

## Impact of ultraviolet radiation nearly overrides the effects of elevated $p\text{CO}_2$ on a prominent nitrogen-fixing cyanobacterium

Xiangqi Yi <sup>1</sup>, Kunshan Gao <sup>1,2\*</sup>

<sup>1</sup>State Key Laboratory of Marine Environmental Science, College of the Environment and Ecology, Xiamen University, Xiamen, China

<sup>2</sup>Co-Innovation Center of Jiangsu Marine Bio-industry Technology, Jiangsu Ocean University, Lianyungang, China

### Abstract

Although the marine  $\text{N}_2$ -fixers *Trichodesmium* spp. are affected by increasing  $p\text{CO}_2$  and by ultraviolet radiation (UVR) in their habitats, little is known on their potential responses to future ocean acidification in the presence of UVR. We grew *Trichodesmium* at two  $p\text{CO}_2$  levels (410 and 1000  $\mu\text{atm}$ ) under natural sunlight, documented the filament length, growth, and chlorophyll content after its acclimation to the  $p\text{CO}_2$  treatments, and measured its carbon and  $\text{N}_2$  fixation rates under different solar radiation treatments with or without UVR. We showed that the elevated  $p\text{CO}_2$  did not significantly alter the diazotroph's growth, filament length, or pigment content, and its photosynthetic rate was only affected by solar radiation treatments rather than the  $p\text{CO}_2$  levels. The presence of UV-A and UV-B inhibited photosynthesis by 10–22% and 17–21%, respectively. Inhibition of  $\text{N}_2$  fixation by UV-B was proportional to its intensity, whereas UV-A stimulated  $\text{N}_2$  fixation at low, but inhibited it at high, intensities. Elevated  $p\text{CO}_2$  only stimulated  $\text{N}_2$  fixation under moderate levels of solar radiation. The simulated depth profile of  $\text{N}_2$  fixation in the water column showed that UV-induced inhibition dominated the combined effects of elevated  $p\text{CO}_2$  and UVR at 0–30 m depth and the combination of these factors enhanced  $\text{N}_2$  fixation at 30–60 m depth, but this effect diminished in deeper water. Our results suggest that *Trichodesmium* could be influenced more by UVR than by  $p\text{CO}_2$  and their combined action result in negative effects on  $\text{N}_2$  fixation under high solar radiation, but positive effects under low to moderate solar radiation.

The filamentous cyanobacterium *Trichodesmium* is one of the most common  $\text{N}_2$ -fixing organisms (diazotrophs) in the pelagic oceans (Capone et al. 1997; Zehr 2011; Zehr and Capone 2020). Its latitudinal distribution is roughly limited to waters between the 20°C isotherms of the annual mean sea surface temperature, approximately corresponding to the area between 30°N and 30°S (LaRoche and Breitbarth 2005; Luo et al. 2014; Tang and Cassar 2019). In terms of its vertical distribution in the water column, *Trichodesmium* spp. can be found from the surface to a depth of 150 m, with biomass maxima usually occurring at depths of 20–40 m (Capone et al. 1997; Rouco et al. 2016), which exposes the cells to solar irradiances including ultraviolet radiation (UVR, 280–400 nm) the effects of which have often been neglected in

oceanographic surveys (Gao et al. 2020). *Trichodesmium* has been shown to form extensive blooms, during which large quantities of biomass conglomerate in surface layer (Westberry and Siegel 2006). Since *Trichodesmium* is one of the most ecologically and biogeochemically significant diazotrophs (Capone et al. 1997; Bergman et al. 2013), contributing about 50% of oceanic  $\text{N}_2$  fixation (Capone et al. 2005; LaRoche and Breitbarth 2005), its responses to ocean global changes are of general and increasing concern.

As biological  $\text{N}_2$  fixation by *Trichodesmium* occurs in the light and directly relies on the energy and reductant generated by photosynthesis (Chen et al. 1996; Berman-Frank et al. 2001), light is the key environmental driver regulating its physiological performance (Breitbarth et al. 2008; Goebel et al. 2008; Cai et al. 2015) and also influences its responses to changes in temperature (Yi et al. 2020),  $\text{CO}_2$  (Kranz et al. 2010; Garcia et al. 2011) and micronutrient availability (Rodriguez and Ho 2014). To drive photosynthesis, photoautotrophs mainly utilize photosynthetically active radiation (400–700 nm, PAR), but they are often inevitably exposed to harmful UVR. Although UV-B radiation (280–315 nm) accounts for less than 1% of incident solar radiation in most regions of the world, it is usually more harmful for photosynthetic organisms

\*Correspondence: ksgao@xmu.edu.cn

Additional Supporting Information may be found in the online version of this article.

**Author Contribution Statement:** X.Y. and K.G. designed the experiment. X.Y. carried out the experiment. X.Y. and K.G. analyzed the data and wrote the manuscript.

than UV-A (315–400 nm) in terms of biologically weighted impacts, as UV-B photons are more photobiologically active than UV-A which is about 6–8% of the total solar energy in tropical and subtropical regions (Gao et al. 2022). It has been documented that solar UVR can penetrate to 80 m deep in the pelagic region of oceans (Piazana et al. 2002; Tedetti et al. 2007). One of the main targets of UV-B is DNA, which can be photo-transformed to thymine–thymine pyrimidine–pyrimidone photoproducts and cyclobutane pyrimidine dimers (Häder et al. 2015; Pathak et al. 2019). These lesions result in serious structural distortions of DNA molecules and retard DNA replication and transcription, triggering cell death under extreme situations (Häder et al. 2015; Pathak et al. 2019). For phototrophs, the direct absorption of UVR by the Mn cluster in photosystem (PS) II leads to damage to the central PSII protein D1 (Hakala et al. 2005; Ohnishi et al. 2005). In addition, UVR can cause indirect damage via inducing the production of reactive oxygen species (ROS), causing the breakage of single- and/or double-stranded DNA (Rastogi et al. 2010a). On the other hand, positive effects of low to moderate levels of UVR have also been reported in phytoplankton, including enhancing photosynthetic carbon fixation (Gao et al. 2007), increasing the activity of PS I (Chen et al. 2020), stimulating  $\text{CO}_2$  concentrating mechanisms (Gao et al. 2021) and improving growth and biomass production (Wu et al. 2005a). Since *Trichodesmium* spp. are distributed across a range of depth and latitudes, their cells are exposed to changing levels of UV-A and UV-B due to spatiotemporal changes in levels of solar radiation and meteorological conditions. However, the effects of UVR on *Trichodesmium* have been rarely examined (Cai et al. 2017; Zhu et al. 2020). In field studies particularly, UV effects are often unconsciously neglected, as the standard vessels (polycarbonate or glass bottles) used for *Trichodesmium* incubation experiments are almost opaque to UVR. Such neglect could significantly bias the estimates of  $\text{N}_2$  fixation by *Trichodesmium* (Cai et al. 2017; Zhu et al. 2020).

On the other hand, progressive ocean acidification caused by anthropogenic emissions of  $\text{CO}_2$  is suggested to impact marine organisms (Doney et al. 2020), since it alters seawater carbonate chemistry by decreasing pH and  $\text{CO}_3^{2-}$  and increasing levels of  $\text{CO}_2$  and  $\text{HCO}_3^-$ . A number of reports in the literature have shown that *Trichodesmium* can benefit from the increased availability of  $\text{CO}_2$  and  $\text{HCO}_3^-$  (Levitan et al. 2007; Hutchins et al. 2009; Boatman et al. 2018), whereas several other studies have reported that lowered pH reduced *Trichodesmium* growth and  $\text{N}_2$  fixation, especially under iron limitation (Shi et al. 2012; Hong et al. 2017). Although such inconsistency is yet to be reconciled (Hutchins et al. 2017; Shi et al. 2017), the potential UV effects have not yet been incorporated into examination of the effects of ocean acidification on *Trichodesmium*. In addition, it is predicted that ocean warming would increase shoaling of the upper mixing layer in the subtropical central gyres where *Trichodesmium* is primarily found, thus substantially increasing its exposure to

UVR (Gao et al. 2012). In the foreseeable future, *Trichodesmium*, along with other phytoplankton species in the upper mixing layer, will have to deal with acidified seawater under the influence of multiple drivers including UVR (Boyd et al. 2018). Therefore, exploring the combined effects of UVR and elevated  $p\text{CO}_2$  on *Trichodesmium* can not only improve the estimates of its  $\text{N}_2$  fixation in contemporary oceans, but also provide new knowledge toward understanding its responses to future ocean changes.

Here, we grew the *Trichodesmium erythraeum* IMS 101 at two  $p\text{CO}_2$  treatments (410  $\mu\text{atm}$  vs. 1000  $\mu\text{atm}$ ) under the full-spectrum solar radiation (including UVR) and documented its filament length, growth, pigment content, photosynthesis, and light response curves of  $\text{N}_2$  fixation. Compared to previous studies exploring UV effects on *Trichodesmium* (Cai et al. 2017; Zhu et al. 2020), this study not only investigated the combined effects of elevated  $p\text{CO}_2$  and UVR under natural solar radiation, but measured the  $\text{N}_2$  fixation rates under a gradient of PAR and UVR rather than at a fixed intensity, which will facilitate the evaluation of UVR effects under more realistic and dynamic sunlight conditions. Our results suggest that UVR is a more influential factor than  $p\text{CO}_2$  for *Trichodesmium* and its impacts are spectrum and intensity dependent.

## Materials

### Experimental setups and culture conditions

The *Trichodesmium* strain (*T. erythraeum* IMS 101) was originally isolated from the North Atlantic Ocean (Prufert-Bebout et al. 1993). Because it was logistically difficult to maintain the cultures in outdoor conditions, we started the acclimation to different  $p\text{CO}_2$  treatments in the laboratory. *Trichodesmium* cells were grown in artificial seawater YBCII without combined nitrogen (Chen et al. 1996) at  $27 \pm 1^\circ\text{C}$ . The cultures were maintained under a 12 : 12 h light/dark cycle (light period: 08 : 00 to 20 : 00 local time) with white-light LEDs (ST5-LED10, FLS) as the light source (emitting no UVR). The light intensity during the light period was constant at  $150 \pm 20 \mu\text{mol photons m}^{-2} \text{ s}^{-1}$ . Two  $p\text{CO}_2$  treatments, ambient ( $p\text{CO}_2$  410  $\mu\text{atm}$ ; referred to as AC) and elevated ( $p\text{CO}_2$  1000  $\mu\text{atm}$ ; referred to as HC), were set up by bubbling outdoor air or  $\text{CO}_2$ -air mixtures with the target  $\text{CO}_2$  partial pressures using a commercial  $\text{CO}_2$  enriching device (CE100D, Ruihua). The elevated  $p\text{CO}_2$  level was selected based on the projection for 2100 under the RCP8.5 scenario (Stocker et al. 2013). The bubbling also helped to keep the cells grow in the form of filaments without forming colonies. Three biological replicates were used for each  $p\text{CO}_2$  treatment. The cultures were diluted every 4–7 d to maintain the cells in exponential growth phase. The  $\text{pH}_{\text{NBS}}$  of the culture medium was measured using a calibrated Benchtop pH meter (Orion Star A211, Thermo Scientific) equipped with a combination pH electrode (Orion 8102BN ROSS, Thermo Scientific), and the total alkalinity (TA) was determined using a TA titrator

(AS-ALK+, Apollo SciTech). Other parameters of the carbonate chemistry for the culture medium, including dissolved inorganic carbon (DIC) and  $p\text{CO}_2$ , were calculated from the values of  $\text{pH}_{\text{NBS}}$  and TA using CO2SYS (version 2.3) (Supporting Information Table S1). The changes in the carbonate chemistry parameters were documented before and after diluting the cultures, with a  $\text{pH}_{\text{NBS}}$  change less than 0.09, and there was a significant  $\text{pH}_{\text{NBS}}$  difference between the AC and HC treatments (Supporting Information Table S1). Chlorophyll *a* (Chl *a*) concentration was measured at every dilution (see the next section). The independent cultures were allowed to acclimate to different  $p\text{CO}_2$  levels for at least 10 generations, during which stable specific growth rates were achieved (see the following section).

Subsequently, the cultures were moved outdoors to be exposed to full-spectrum solar radiation (including the presence of UVR). From this point, quartz vessels (which allow transmission of UVR) were used for the cultures. They were placed in a water bath for temperature control and covered by one layer of neutral density filter (60% transmission). The sunlight level to which the cells were exposed were close to that at a depth of  $\sim 20$  m in the open ocean, where maximal biomass density of *Trichodesmium* has been observed (Capone et al. 1997). The side walls of the water bath were low enough ( $\sim 20$  cm tall) that they did not block the sunlight during the daytime. The actual temperatures in the water bath varied between  $26^\circ\text{C}$  and  $28^\circ\text{C}$  and were continuously monitored by a portable CTD (RBR concerto, Canada). The AC and HC treatments were achieved in the same way as described for the indoor cultures, with a semi-continuous mode of dilution in order to maintain carbonate chemistry stability. Incident solar radiation (PAR, UV-A, and UV-B) during the experimental period was continuously monitored with a broadband radiometer (MS-212A/MS-212W/ML-020P, EKO) which recorded the data every minute. The radiometer was installed on the roof of our laboratory building which was  $< 25$  m from the ground. The actual PAR received by the cells in different vessels (and tubes or vials used for measurements of carbon and  $\text{N}_2$  fixations) was checked by a spherical micro quantum sensor (US-SQS/WB, Walz), which could be inserted into the incubation vessels. The cells were acclimated to the outdoor sunlit conditions for 2 weeks (03 January 2019 to 17 January 2019,  $\sim$  six generations) during which the photoperiod was from 06 : 50 to 17 : 30 (local time). We then started sampling and data collection (see Supporting Information Fig. S1 for the details, including daily doses of the irradiances and sampling timing).

#### Chl *a*, filament abundance and length, and specific growth rate

Chl *a* concentration was spectrophotometrically quantified by gently filtering the cells onto glass-fiber filters (25 mm, GF/F, Whatman), followed by extraction in pure methanol at

$4^\circ\text{C}$  for 24 h and centrifugation at 6000g for 10 min. The absorbance spectrum of the supernatant was determined using a spectrophotometer (DU800, Beckman). Chl *a* concentration was calculated as described by Ritchie (2006):

$$[\text{Chl } a \text{ } (\mu\text{g mL}^{-1})] = 12.9447 \times (A_{665} - A_{750}),$$

where  $A_{665}$  and  $A_{750}$  indicate the absorbances at 665 and 750 nm, respectively.

We measured the filament abundance and length using an inverted microscope fitted with a camera (TS100-F, Nikon). The filament number and the length of each filament in a known volume (50–100  $\mu\text{L}$ ) of culture were measured, and this was repeated 3–5 times for each culture. The boundaries between the cells in the trichomes were ambiguous under the microscope, so we were unable to normalize the content of Chl *a* and the rates of  $\text{N}_2$  fixation and carbon fixation to cell number. The Chl *a* concentration and total filament length (calculated by adding together the length of each measured filament) were used as the proxies for biomass to calculate the specific growth rate ( $\mu$ ), respectively:

$$\mu \text{ (d}^{-1}\text{)} = \frac{\ln m_2 - \ln m_1}{t_2 - t_1},$$

where  $m_2$  and  $m_1$  are the biomass values at time  $t_2$  and  $t_1$ .

#### Photosynthetic carbon fixation

A subsample ( $\sim 200$  mL) was drawn from each vessel to determine photosynthetic carbon fixation by the  $^{14}\text{C}$  method. The subsample was dispensed into 50-mL quartz tubes, and 100  $\mu\text{L}$  of  $\text{NaH}^{14}\text{CO}_3$  solution (ICN Radiochemicals) with radioactivity of  $\sim 5 \mu\text{Ci}$  (0.185 MBq) was added to each tube. The tubes were then exposed to 60% solar radiation (one layer of neutral density filter) for 2 h around noon under three different treatments: (a) PAB, receiving full-spectrum solar radiation (PAR + UV-A + UV-B); (b) PA, receiving solar irradiances above 320 nm (PAR + UV-A, quartz tubes wrapped in Folex 320 film with 50% transmission at 320 nm); and (c) PAR, receiving solar radiation above 395 nm (PAR alone treatment, quartz tubes wrapped in Ultraphan 395 film with 50% transmission at 395 nm). For each vessel, one more tube was wrapped in aluminum foil to act as a dark treatment. After the 2 h incubation, subsamples were filtered onto glass-fiber filters (25 mm, GF/F, Whatman) and preserved at  $-20^\circ\text{C}$ . Upon further analysis, GF/F filters were placed in 20-mL scintillation vials, exposed to HCl fumes for 12 h and dried for 6 h to remove unincorporated inorganic  $^{14}\text{C}$ . Scintillation cocktail (5 mL, Hisafe 3, Perkin-Elmer) was then added to immerse the GF/F filter. The incorporated radioactivity (counts per minute [CPM]) was measured by a liquid scintillation counter (LC 6500, Beckman Coulter). Photosynthetic carbon fixation rate was calculated as:

$$\text{Carbon fixation} = \frac{1.06 \times \text{DIC} \times (\text{DPM}_L - \text{DPM}_D)}{\text{DPM}_{\text{tot}} \times t},$$

where  $\text{DPM}_D$  and  $\text{DPM}_L$  refer to DPM (disintegrations per minute), calculated from the CPM using the external standard and channel ratio method, for dark and light (PAR, PA, or PAB) treatments, respectively,  $\text{DPM}_{\text{tot}}$  is the total activity of  $\text{NaH}^{14}\text{CO}_3$  added to the incubation tube,  $t$  is the incubation time and the factor 1.06 is used to correct for the isotopic discrimination between  $^{14}\text{C}$  and  $^{12}\text{C}$ . The radioactivity of a small amount of  $\text{NaH}^{14}\text{CO}_3$  solution mixed with ethanolamine was measured to estimate the value of  $\text{DPM}_{\text{tot}}$ .

### Diazotrophy-light curves

The  $\text{N}_2$  fixation rate was determined using the acetylene reduction assay (Capone 1993) with a gas chromatograph equipped with a flame ionization detector (Clarus 580, PerkinElmer). A ratio of 4 : 1 was used to convert ethylene production to  $\text{N}_2$  fixation. To obtain the light response curve for  $\text{N}_2$  fixation (diazotrophy-light curve), a subsample ( $\sim 120$  mL) was drawn from each vessel and dispensed to 13 mL gas-tight borosilicate glass (UV-transparent, Cai et al. 2017) vials (5 mL culture). Eighteen vials were evenly separated into three groups for different solar radiation treatments: (a) PAB (PAR + UV-A + B), (b) PA (PAR + UV-A), and (c) PAR. The different solar radiation treatments were achieved in the same way as described above for the measurements of photosynthetic carbon fixation. Superimposed on these treatments, six intensity levels (100%, 60%, 36%, 22%, 13%, and 8%) of the incident solar radiation were achieved by covering the vials with different layers of neutral density filters. After 1 mL of air was extracted from the headspace, 1 mL acetylene was added to each vial to start the incubation. Incubation lasted for 2 h around noon and was terminated by the addition of 100  $\mu\text{L}$  saturated HgCl solution. For the three vials used as blanks, saturated HgCl solution was immediately added after the injection of acetylene. The average 100% incident PAR, UV-A, and UV-B during the measurements of photosynthetic carbon fixation and  $\text{N}_2$  fixation were 921.2  $\mu\text{mol photons m}^{-2} \text{ s}^{-1}$  ( $\sim 200.3 \text{ W m}^{-2}$ ), 24.5 and 0.85  $\text{W m}^{-2}$ , respectively. Both photosynthetic carbon fixation and  $\text{N}_2$  fixation rates were normalized to Chl *a*, and it was reasonable to assume that the cellular Chl *a* content had not been altered by the different treatments during the 2 h measurements (Cai et al. 2017).

### Quantification of UV effects

Based on the rates of  $\text{N}_2$  fixation or photosynthetic carbon fixation measured under different solar radiation treatments with or without UVR, the UV-induced inhibition values were evaluated as follows:

$$E_{\text{UVR}} = \frac{A_{\text{PAR}} - A_{\text{PAB}}}{A_{\text{PAR}}} \times 100\%,$$

$$E_{\text{UVA}} = \frac{A_{\text{PAR}} - A_{\text{PA}}}{A_{\text{PAR}}} \times 100\%,$$

$$E_{\text{UVB}} = E_{\text{UVR}} - E_{\text{UVA}},$$

where  $E_{\text{UVR}}$ ,  $E_{\text{UVA}}$ , and  $E_{\text{UVB}}$  represent the inhibitions by UVR, UV-A, and UV-B, respectively, and  $A_{\text{PAB}}$ ,  $A_{\text{PA}}$ , and  $A_{\text{PAR}}$  indicate  $\text{N}_2$  fixation rates or photosynthetic carbon fixation rates determined under the corresponding solar radiation treatments.

### Statistical analysis

All statistical analyses and data visualization were carried out using R (version 4.1.1) and packages “mgcv (version 1.8-38),” “car (version 3.0-11),” “MASS” (version 7.3-54), “tibble (version 3.1.5),” “ggplot2 (version 3.1.5),” “tidyr (version 1.1.4),” “readr (version 2.0.2),” “purrr (version 0.3.4),” “dplyr (version 1.0.7),” “ggtext (version 0.1.1),” and “ggpubr (version 0.4.0).” The significant differences in specific growth rate and Chl *a* content between AC and HC treatments were tested by a Student’s *t*-test. The homogeneity of variance in filament length between the treatments was tested by Levene’s test and Fligner–Killen test. In addition, to test the  $p\text{CO}_2$  effects on the mean filament length, we built a linear mixed-effects model with fixed effects being the  $p\text{CO}_2$  treatments and random effects on the intercept by independent cultures. For analyzing the combined effects of  $p\text{CO}_2$  and solar radiation treatments on the photosynthetic carbon fixation rate, we started from building a linear mixed-effects model with  $p\text{CO}_2$  treatment (AC vs. HC), solar radiation treatment (PAR vs. PA vs. PAB) and their interaction as fixed effects and with random effects by independent cultures on the intercept. Afterward, we followed the step-down strategy (Zuur et al. 2009) to optimize the model. Generalized additive models (GAMs) were built to analyze the diazotrophy-light curves. The effects of PAR, UV-A, and UV-B on  $\text{N}_2$  fixation were expressed by smooth functions or linear functions. If two smooth/linear functions were needed to separately describe the PAR/UV-A/UV-B effects under AC and HC treatments, there existed interactive effects between  $p\text{CO}_2$  and PAR/UV-A/UV-B. The building, selection, and validation of statistical models follow the guidelines and principles provided in Pinheiro and Bates (2006), Zuur et al. (2009), and Wood (2017). Significance was determined at the 0.05 level. The maximum  $\text{N}_2$  fixation rate ( $\text{Nfix}_{\text{max}}$ ) and the corresponding optimal PAR ( $\text{PAR}_{\text{opt}}$ ) were derived from the GAMs. To obtain the 95% confidence intervals for  $\text{Nfix}_{\text{max}}$  and  $\text{PAR}_{\text{opt}}$ , we carried out 10,000 simulations from the posterior distribution of the GAMs. In addition, the finite difference method was used to analyze the slopes of the diazotrophy-light curves at low ( $\alpha$ ) and high ( $\beta$ ) levels of PAR. The parameter  $\alpha$  indicates the apparent light use efficiency under the light-limiting conditions, and  $\beta$  reflects the inhibition slope under high light levels beyond the saturation point.

The confidence intervals for  $\alpha$  and  $\beta$  were also provided by the posterior simulations from the fitted GAMs.

## Results

### Specific growth rate and filament length

The specific growth rates of the *Trichodesmium* cells grown indoors under AC and HC treatments were  $0.46 \pm 0.01$  and  $0.43 \pm 0.01 \text{d}^{-1}$ , respectively (Fig. 1a), reflecting that the elevated  $p\text{CO}_2$  suppressed the growth rate by about 6% (Student's  $t$ -test,  $df = 4$ ,  $p < 0.01$ ) after acclimation for 10 generations. After the cultures were transferred to outdoors and exposed to full-spectrum solar radiation in the presence of UVR, growth of *Trichodesmium* substantially decreased by  $\sim 65\%$  to  $0.16 \pm 0.06 \text{d}^{-1}$  under AC and by  $\sim 67\%$  to  $0.14 \pm 0.06 \text{d}^{-1}$  under HC, respectively (Fig. 1a; Paired  $t$ -test,  $df = 5$ ,  $p < 0.01$ ), and no significant difference between growth under the two  $p\text{CO}_2$  levels was observed (Student's  $t$ -test,  $df = 4$ ,  $p = 0.749$ ).

The lengths of the measured filaments fell in the range 29.1–388.4  $\mu\text{m}$  with median and mean being 194.2 and 189.8  $\mu\text{m}$ , respectively (Fig. 1b; Supporting Information

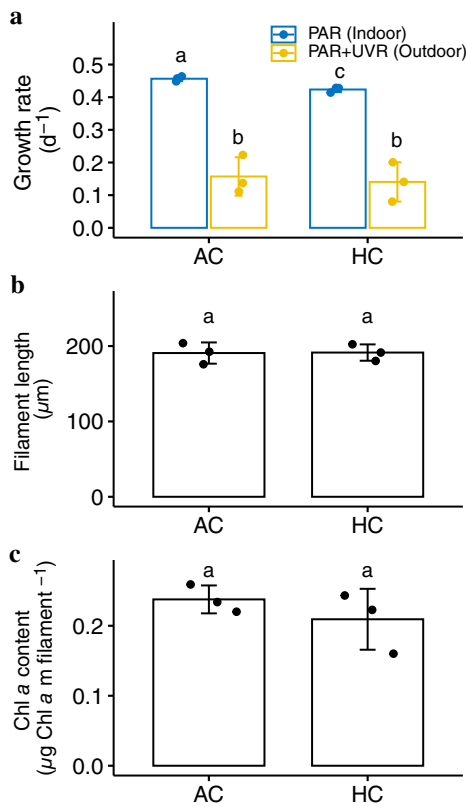


**Fig. 1.** (a) Specific growth rates obtained under sunlit condition with UVR and those obtained during indoor growth without UVR, (b) average filament length, and (c) Chl *a* content of *Trichodesmium* IMS 101 grown at AC ( $410 \mu\text{atm}$ ) and HC ( $1000 \mu\text{atm}$ ). The bars were the means of triplicates  $\pm$  standard deviation, and the points were the values for each independent culture. The different letters above the bars mark significant differences between the treatments ( $p < 0.05$ ).

Fig. S2). There was no indication that the variance in filament length was significantly different among the six independent cultures (Levene's test,  $F_{5,577} = 1.73$ ,  $p = 0.13$ ). Similarly, the variance in filament length was not significantly different between the two  $p\text{CO}_2$  treatments (Levene's test,  $F_{1,581} = 2.44$ ,  $p = 0.12$ ). The homogeneity of variance in filament length was further confirmed by the Fligner–Killeen test. Analysis based on the linear mixed-effects model showed that the elevated  $p\text{CO}_2$  did not bring about any significant effect on the mean filament length ( $F_{1,4} = 4.522$ ,  $p = 0.10$ ). In addition, the standard deviation of random effect was much less than the within-group standard error and there was considerable imprecision in the estimate of standard deviation of the random effect, both of which indicated that including the random effect was unnecessary. Reanalysis of the data using a linear model also resulted in insignificant effects of HC in contrast to AC ( $F_{1,582} = 0.191$ ,  $p = 0.66$ ). Therefore, our results showed that the filament length was not significantly influenced by the elevated  $p\text{CO}_2$ . The Chl *a* contents in the AC and HC-grown cells were  $0.24 \pm 0.02$  and  $0.21 \pm 0.04 \mu\text{g Chl a per meter of filament length}$  (Fig. 1c), respectively. Again, no significant  $p\text{CO}_2$  effect was detected (Student's  $t$ -test,  $df = 4$ ,  $p = 0.16$ ).

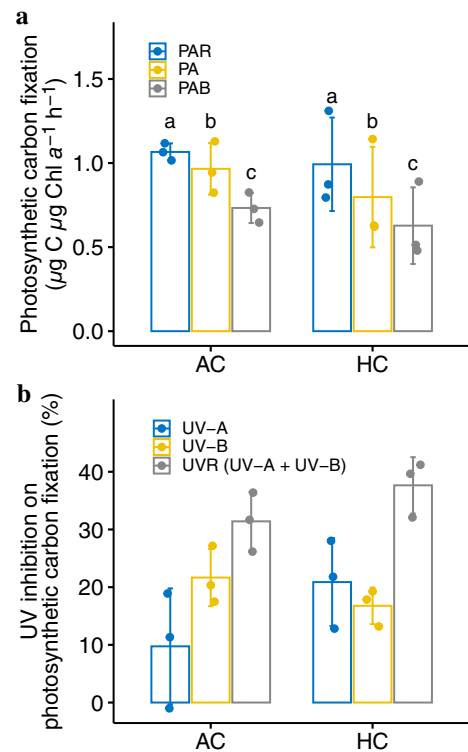


**Fig. 2.** (a) The photosynthetic carbon fixation rates measured under different solar radiation treatments (PAR; PA: PAR + UV-A; PAB: PAR + UV-A + B) and (b) the UV-induced inhibitions in *Trichodesmium* IMS 101 cells grown at AC ( $410 \mu\text{atm}$ ) and HC ( $1000 \mu\text{atm}$ ) conditions. Values are means of triplicates  $\pm$  standard deviation. The different letters above the bars mark significant differences between the treatments ( $p < 0.05$ ).

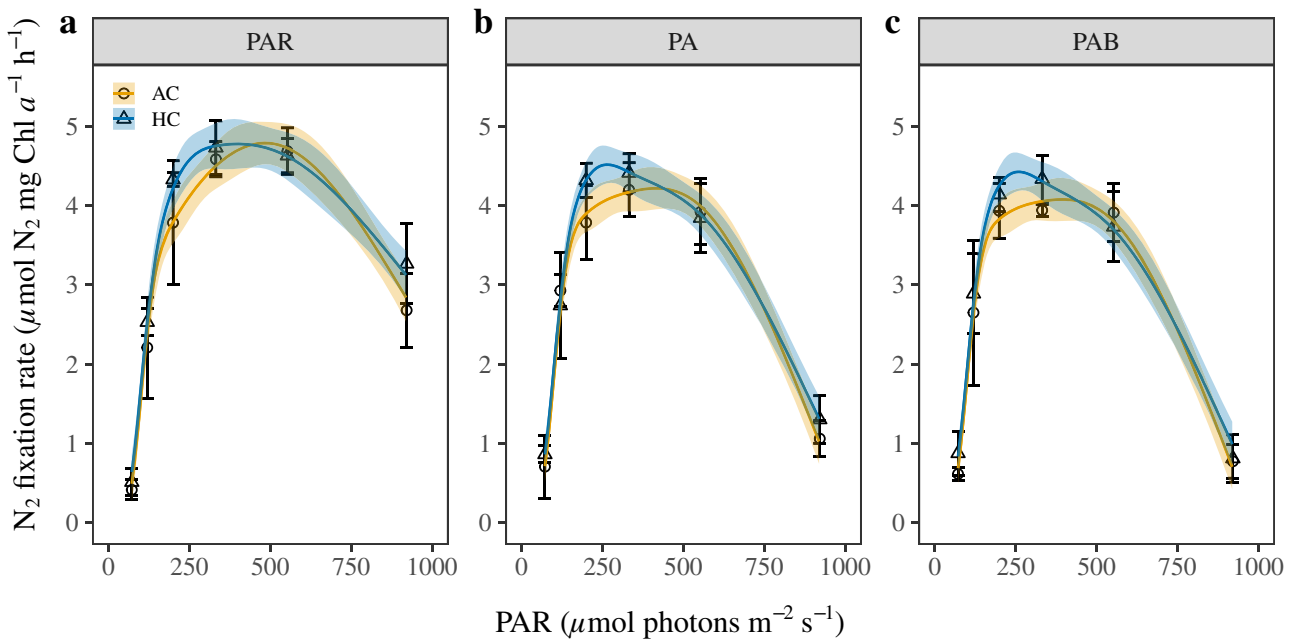


**Fig. 3.** Diazotrophy-light curves measured under PAR (a), PA (PAR + UV-A) (b), and PAB (PAR + UV-A + UV-B) (c) for *Trichodesmium* IMS 101 grown under AC (410  $\mu\text{atm}$ ) and HC (1000  $\mu\text{atm}$ ) conditions. Values are means of triplicates  $\pm$  standard deviation. Lines with shadow represents the predicted mean  $\pm 1.96 \times \text{SE}$  of the GAM.

**Table 1.** The apparent light use efficiency ( $\alpha$ ) and photoinhibition efficiency ( $\beta$ ) for  $\text{N}_2$  fixation, the maximal rates of  $\text{N}_2$  fixation and corresponding optimal PAR determined under solar radiation treatment PAR, PA (PAR + UV-A) and PAB (PAR + UV-A + UV-B) for *Trichodesmium* IMS 101 grown under AC (410  $\mu\text{atm}$ ) and HC (1000  $\mu\text{atm}$ ) conditions. Values are 95% confidence intervals. The unit for  $\alpha$  and  $\beta$  are  $\mu\text{mol N}_2 \text{ mg Chl a}^{-1} \text{ h}^{-1} (\mu\text{mol photons m}^{-2} \text{ s}^{-1})^{-1}$ , the unit for  $\text{Nfix}_{\text{max}}$  is  $\mu\text{mol N}_2 \text{ mg Chl a}^{-1} \text{ h}^{-1}$ , and the unit for  $\text{PAR}_{\text{opt}}$  is  $\mu\text{mol photons m}^{-2} \text{ s}^{-1}$ .

	AC			HC		
	PAR	PA	PAB	PAR	PA	PAB
$\alpha$	[0.0237, 0.0314]	[0.0262, 0.0336]	[0.0259, 0.0333]	[0.0239, 0.0315]	[0.0263, 0.0338]	[0.0260, 0.0334]
$\beta$	[0.0046, 0.0090]	[0.0085, 0.0121]	[0.0089, 0.0125]	[0.0029, 0.0073]	[0.0068, 0.0104]	[0.0071, 0.0107]
$\text{Nfix}_{\text{max}}$	[4.55, 5.09]	[4.03, 4.49]	[3.91, 4.36]	[4.58, 5.11]	[4.32, 4.77]	[4.22, 4.68]
$\text{PAR}_{\text{opt}}$	[408.1, 558.5]	[244.7, 504.0]	[236.9, 487.1]	[266.7, 549.2]	[235.6, 355.6]	[232.4, 342.9]

### Photosynthetic carbon fixation

When the photosynthetic carbon fixation rates measured under different solar radiation treatments were compared, it was obvious that removal of UV-B increased, and removal of both UV-A and UV-B further increased, the photosynthetic carbon fixation rates, regardless of the  $p\text{CO}_2$  levels (Fig. 2a). UV-A inhibited photosynthesis by  $\sim 10\%$  under AC and by  $\sim 21\%$  under HC, respectively. UV-B inhibited photosynthesis by  $\sim 22\%$  under AC and by  $\sim 17\%$  under HC, respectively (Fig. 2b). Analysis based on the linear mixed-effects model confirmed such observations, that is, the photosynthetic carbon fixation was significantly affected by the solar radiation treatment ( $F_{2,10} = 30.6$ ,  $p < 0.005$ ) but not by  $p\text{CO}_2$  levels and their interactions.

### Diazotrophy-light curves

The light response curves of  $\text{N}_2$  fixation rate (diazotrophy-light curves) determined in the presence or absence of UVR showed similar and typical traits with light-limiting, saturating and inhibiting phases in the cells grown at the two  $p\text{CO}_2$  levels (Fig. 3). The presence of UVR significantly reduced the maximal rates of  $\text{N}_2$  fixation ( $\text{Nfix}_{\text{max}}$ ) and brought about a sharper decline ( $\beta$ ) of the rates under supraoptimal levels of solar radiation (Fig. 3; Table 1). The apparent light use efficiency ( $\alpha$ ) and the optimal PAR ( $\text{PAR}_{\text{opt}}$ ) were not significantly affected by  $p\text{CO}_2$  levels or solar radiation treatments (Table 1). The UV-induced inhibition was as much as 70% at the highest levels of solar radiation (Fig. 4a). Comparison of the percentage inhibition of  $\text{N}_2$  fixation by UV-A and UV-B (Fig. 4b)

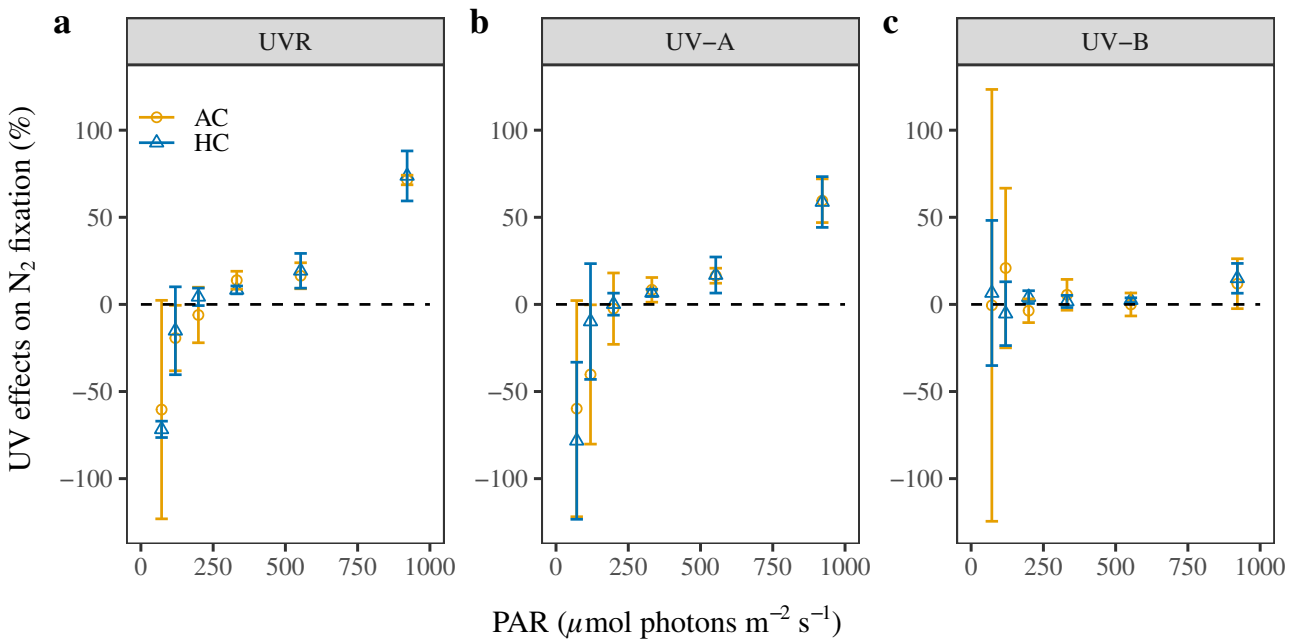


**Fig. 4.** Effects of UV-R (a), UV-A (b), and UV-B (c) on the N<sub>2</sub> fixation rates of *Trichodesmium* IMS 101 grown under AC (410 μatm) and HC (1000 μatm) conditions. Values above 0 represent inhibitive effects, and values below 0 represents stimulative effects.

indicated that UV-A dominated the UV effects, and the effect tended to be stimulatory (negative values) at low to moderate, but to be inhibitory (positive values) at high levels of solar radiation. Analyses based on the GAM analysis indicated that the UV-B-induced inhibition was significant and proportional to its intensity ( $p < 0.05$ ), though its extent was relatively small. Additionally, there were interactive effects between  $p\text{CO}_2$  and PAR, which were mainly reflected as the enhancement of N<sub>2</sub> fixation by elevated  $p\text{CO}_2$  at medium levels of solar radiation (Fig. 3). No interactive effect between  $p\text{CO}_2$  and UV-A/UV-B was detected by the GAM.

Based on the GAM analyses and typical values of the attenuation coefficients for PAR (0.03 m<sup>-1</sup>), UV-A (0.05 m<sup>-1</sup>), and UV-B (0.13 m<sup>-1</sup>) (Tedetti et al. 2007) in pelagic oceans, we established the depth profiles of N<sub>2</sub> fixation by *Trichodesmium* under two conditions: AC + PAR vs. HC + PAR + UVR (Fig. 5). At depths less than 30 m, where solar radiation was relatively strong, the difference between the two conditions mainly came from the UV-induced inhibition of N<sub>2</sub> fixation. As the depth increases, the stimulative effects of the elevated  $p\text{CO}_2$  and UVR at moderate solar radiation were responsible for the difference. Finally, at depths over 60 m, there was no significant difference between the two conditions.

### Discussion

*Trichodesmium* is widely distributed throughout the oligotrophic tropical and subtropical oceans, being exposed to varying levels of solar UVR. Our results indicated that both N<sub>2</sub> fixation and photosynthesis of *Trichodesmium* IMS 101 were

significantly affected by UVR (Figs. 2, 3). In particular, the UV effects appeared to be both spectrum and intensity dependent. In addition, the diazotrophy-light curve was affected by both  $p\text{CO}_2$  levels and solar radiation treatment (Figs. 3, 4), whereas elevated  $p\text{CO}_2$  showed no significant impact on *Trichodesmium* growth, filament length, Chl *a* content (Fig. 1) and photosynthetic carbon fixation (Fig. 2). The simulation of combined effects of UVR and elevated  $p\text{CO}_2$  on the depth profile of N<sub>2</sub> fixation (Fig. 5) showed that the inhibition by UVR dominated the combined effects at shallow depths (0–30 m) with inhibition up to 66% at the surface, the combination of UV and elevated  $p\text{CO}_2$  enhanced N<sub>2</sub> fixation at depths of 30–60 m with maximum enhancement by 19% at a depth of 48 m, and such combined effects faded to nil at depths more than 60 m.

The specific growth rate of *Trichodesmium* ranged from 0.2–0.6 d<sup>-1</sup> when grown under laboratory conditions without UV (Hutchins et al. 2007; Shi et al. 2012; Boatman et al. 2017) (Fig. 1a). Growth rate was significantly reduced by up to 65% when exposed to solar radiation with UVR (Fig. 1; Supporting Information Fig. S1). Such relatively slow growth in the presence of UVR was consistent with the estimated doubling time reported from field observations (Mulholland et al. 2006). UVR is known to cause direct and indirect damage to biomacromolecules such as DNA, RNA, proteins, and lipids, including those closely related to photosynthesis and nutrient acquisition (Rastogi et al. 2010a). Simultaneously, these forms of damage can induce corresponding protective and repair mechanisms which can mitigate the harmful impacts of UVR (Raven 2011; Rastogi et al. 2014). For example, a classic type of protective mechanism found in cyanobacteria is increasing

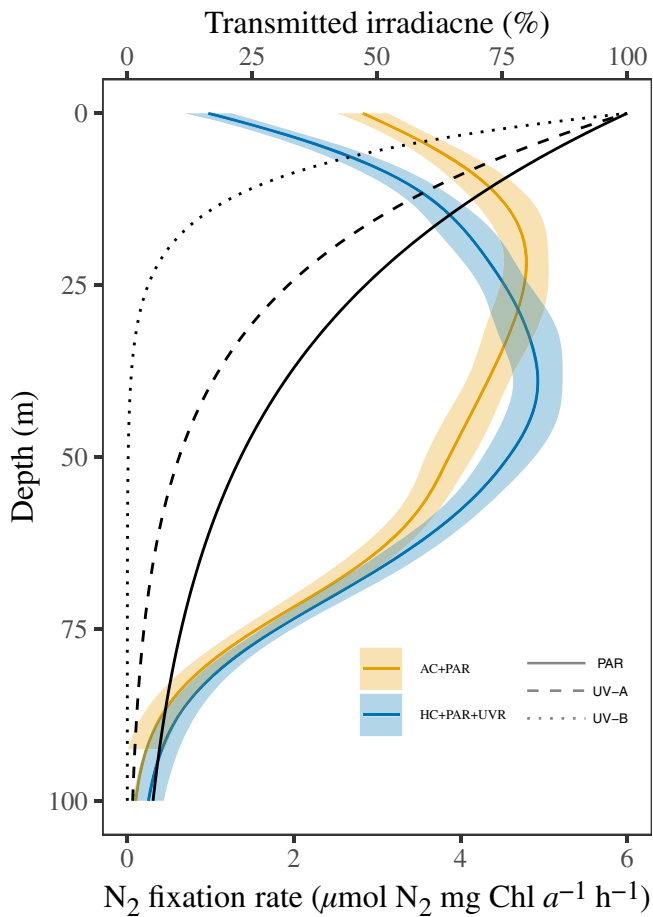


**Fig. 5.** Simulated depth profiles of transmitted irradiances and N<sub>2</sub> fixation by *Trichodesmium* under two conditions: AC + PAR (current condition with methods neglecting presence of UVR; yellow line) vs. HC + PAR + UVR (future pCO<sub>2</sub> at the year 2100 with UVR being considered; blue line). Colored lines with shadow represent the predicted N<sub>2</sub> fixation rates in mean ± 1.96 × SE by the GAM. Black lines represent the transmitted irradiance (percent of the surface incident irradiance).

the synthesis and accumulation of sunscreen substances, such as mycosporine-like amino acids and scytonemin (Gao and Garcia-Pichel 2011; Shang et al. 2018). *Trichodesmium* cells exposed to solar radiation with UVR in this work showed higher absorption in the UV absorption region than those grown under UV-free conditions (Supporting Information Fig. S3), suggesting that increased concentrations of cellular UV-screening compounds could be a mechanism to cope with UV stress in *Trichodesmium*. Since UV-induced damage can impede resource acquisition processes and also raise the cellular demand for resources, both of which can result in reduced growth (Raven 2011), it is likely to be one of the main causes responsible for the low rates of growth reported here and found in field studies (Mulholland et al. 2006).

The length of filaments was reported to be proportional to the specific growth rate in *Trichodesmium* IMS 101 (Cai et al. 2015). In the present work, neither the specific

growth rate nor the filament length was altered by the elevated pCO<sub>2</sub> projected for future ocean acidification under solar radiation with UVR (Fig. 1a,b). In addition, the mean filament length reported here lies at the low end of the commonly observed range (Levitan et al. 2007; Cai et al. 2015; Zhu et al. 2020). Previous studies have shown that exposure to UVR induced breakage of cyanobacterial filaments (Wu et al. 2005b; Rath and Adhikary 2007; Rastogi et al. 2010b). The relatively shorter filaments found in our study might therefore be partially attributable to UV exposure, which might also relate to the high ROS accumulation in the cells exposed to UVR (Rastogi et al. 2010a).

Regardless of the pCO<sub>2</sub> level, the photosynthetic carbon fixation rate of *Trichodesmium* IMS 101 was significantly inhibited by UVR (Fig. 2). This was expected as UVR is known to inhibit photosynthesis across phytoplankton taxa (Häder et al. 2015). Nonetheless, UVR is an environmental driver that is often neglected in field investigations of primary productivity due to use of UV-opaque incubation bottles. This might unknowingly bias estimates for physiological processes. For example, the inclusion of UVR resulted in a 13% downward revision to the depth-integrated photosynthesis at midday by *Prochlorococcus* and *Synechococcus* in their typical habitat (Neale and Thomas 2017). Such UV-related bias can also be expected for studies of N<sub>2</sub> fixation by diazotrophs.

Our results showed that when exposed to 100% midday solar radiation in a subtropical area, addition of UVR inhibited the N<sub>2</sub> fixation rates of *Trichodesmium* IMS 101 by up to 70% (Fig. 4). The fact that the effect of UV-B was almost overwhelmed by that of UV-A could be attributed to the incident intensity of UV-A being ~ 30 times that of UV-B (Supporting Information Fig. S1), though the energy of each quantum photon for the latter is greater than that for the former. Nevertheless, the GAM analysis suggested that the UV-B inhibition on N<sub>2</sub> fixation was proportional to its intensity. UV-B can inactivate cyanobacterial nitrogenase directly (Kumar et al. 2003). Furthermore, the inhibition of photosynthesis in *Trichodesmium* by UV-B (Fig. 2) could indirectly reduce N<sub>2</sub> fixation due to the dependence of N<sub>2</sub> fixation on photosynthetic energy supply. On the other hand, not only was the effect of UV-A more prominent but it was also more complicated than that of UV-B. Direct absorption of UVR by the oxygen-evolving complex induces photodamage (Hakala et al. 2005; Ohnishi et al. 2005), and the UV-induced accumulation of ROS is known to impede repair processes (Nishiyama et al. 2006), both of which can cause inhibition of photosynthesis and N<sub>2</sub> fixation in *Trichodesmium*. On the other hand, based on the absorption spectra of Chl *a* and other pigments, UV-A can be harvested as light energy to drive photosynthesis (Gao et al. 2007), which is likely to drive N<sub>2</sub> fixation in *Trichodesmium*. Simultaneously, ROS accumulation might induce upregulation of the water–water cycles to help scavenge the ROS (Asada 1999; Raven et al. 2020). The water–water cycles in *Trichodesmium* are extremely active, which enhances the supply of ATP and helps maintain the hypoxic micro-environment required for N<sub>2</sub>

fixation (Kana 1993; Milligan et al. 2007). Therefore, the observed UV-A effect on N<sub>2</sub> fixation should be a balance between the inhibitory and stimulatory effects. When solar radiation is relatively low (during twilight periods, cloudy days or at depth), incident UV-A can serve as a supplement to PAR to drive photosynthesis and N<sub>2</sub> fixation and the ROS can be readily scavenged by water–water cycles and hence N<sub>2</sub> fixation could be enhanced (Fig. 5). However, as solar radiation increases to higher levels, energy supply is no longer a bottleneck for N<sub>2</sub> fixation, so the negative effects of UV-A become dominant and measurable. Consequently, under these conditions both UV-A and UV-B result in the inhibition of N<sub>2</sub> fixation.

As sunlight penetrates into the water columns, PAR, UV-A, and UV-B are attenuated exponentially. Such attenuation is wavelength-dependent. Usually, UVR is attenuated more rapidly with depth than PAR, and UV-B is readily attenuated faster than UV-A (Fig. 5). Also, the attenuation of solar radiation by seawater is spatiotemporally different (Tedetti and Sempéré 2006). Therefore, positive and negative effects of UVR can vary from time to time and from place to place. Moreover, the responses of *Trichodesmium* to UVR can be strain-specific (Zhu et al. 2020). These features mean that large-scale or global quantification of the UVR effects on N<sub>2</sub> fixation by *Trichodesmium* is challenging, and UVR effects need to be quantified with a spectral biological weighting function (Cullen et al. 1992).

*Trichodesmium* has been recognized (with high confidence) to be a phytoplankton that could benefit from ocean acidification due to increased availability of CO<sub>2</sub> and HCO<sub>3</sub><sup>-</sup> (Hutchins et al. 2009; Dutkiewicz et al. 2015). However, such conclusions have been challenged by other investigations that reported negative effects of a pH drop on *Trichodesmium* (Shi et al. 2012; Hong et al. 2017; Luo et al. 2019). A decrease in seawater pH would decrease the cytosolic pH, leading to a lower efficiency of the nitrogenase enzyme (Hong et al. 2017). In addition, these contradictory findings might be attributed to use of different light sources, which has not been considered in the literature. Differences in the visible light spectrum may also bring about different responses of the diazotroph to key global change drivers. Our work has provided an insight into the combined effects of UVR and pCO<sub>2</sub>, showing that inclusion of UVR can diminish the effects of CO<sub>2</sub> projected for future ocean acidification. Under high levels of solar radiation (as on a sunny day and/or in shallow water layers), negative effects of UVR dominate the combined effects of UV and elevated pCO<sub>2</sub> on N<sub>2</sub> fixation by *Trichodesmium* in surface waters. With decreased solar radiation on cloudy days or in increased water column depths, the combined effects of UV and elevated pCO<sub>2</sub> appear to enhance N<sub>2</sub> fixation (Fig. 5). Moderate levels of PAR and UVR could stimulate the water–water cycles to supply more ATP for the energy-consuming N<sub>2</sub> fixation. Simultaneously, the removal of ROS by water–water cycles also consumes H<sup>+</sup> (superoxide anion and H<sup>+</sup> are acted upon by superoxide dismutase to generate hydrogen peroxide

and dioxygen) (Asada 1999). This might alleviate the negative effects of cytosolic pH drops caused by seawater pCO<sub>2</sub> elevation. In summary, the integrated column N<sub>2</sub> fixation may thus depend on location and meteorological conditions.

Although UVR affects many photochemical and photobiological processes in sea water, most laboratory and deck incubation experiments have not included it due to use of UV-free light sources or UV-opaque incubation bottles (such as polycarbonate and glass) (Gao et al. 2020). This strongly limits our ability to extrapolate from laboratory and/or incubation-based results to in situ conditions. Therefore, we recommend replacing PC or glass bottles with quartz containers during in situ investigations. Since quartz bottles are relatively costly and fragile, bottles made of cyclic olefin copolymer (Agha et al. 2022) or borosilicate glass (Cai et al. 2017) are UV-transparent and can be considered as an alternative.

#### Data availability statement

All relevant data are within the paper and its Supporting Information file.

#### References

- Agha, A., and others. 2022. A review of cyclic olefin copolymer applications in microfluidics and microdevices. *Macromol. Mater. Eng.* **307**: 2200053.
- Asada, K. 1999. The water–water cycle in chloroplasts: Scavenging of active oxygens and dissipation of excess photons. *Annu. Rev. Plant. Physiol. Plant. Mol. Biol.* **50**: 601–639.
- Bergman, B., G. Sandh, S. Lin, J. Larsson, and E. J. Carpenter. 2013. *Trichodesmium*—A widespread marine cyanobacterium with unusual nitrogen fixation properties. *FEMS Microbiol. Rev.* **37**: 286–302.
- Berman-Frank, I., and others. 2001. Segregation of nitrogen fixation and oxygenic photosynthesis in the marine cyanobacterium *Trichodesmium*. *Science* **294**: 1534–1537.
- Boatman, T. G., T. Lawson, and R. J. Geider. 2017. A key marine diazotroph in a changing ocean: The interacting effects of temperature, CO<sub>2</sub> and light on the growth of *Trichodesmium erythraeum* IMS101. *PLoS One* **12**: e0168796.
- Boatman, T. G., K. Oxborough, M. Gledhill, T. Lawson, and R. J. Geider. 2018. An integrated response of *Trichodesmium erythraeum* IMS101 growth and photo-physiology to iron, CO<sub>2</sub>, and light intensity. *Front. Microbiol.* **9**: 624.
- Boyd, P. W., and others. 2018. Experimental strategies to assess the biological ramifications of multiple drivers of global ocean change—A review. *Global Change Biol.* **24**: 2239–2261.
- Breitbarth, E., J. Wohlers, J. Kläs, J. LaRoche, and I. Peeken. 2008. Nitrogen fixation and growth rates of *Trichodesmium* IMS-101 as a function of light intensity. *Mar. Ecol. Prog. Ser.* **359**: 25–36.

- Cai, X., K. Gao, F. Fu, D. Campbell, J. Beardall, and D. Hutchins. 2015. Electron transport kinetics in the diazotrophic cyanobacterium *Trichodesmium* spp. grown across a range of light levels. *Photosynth. Res.* **124**: 45–56.
- Cai, X., D. A. Hutchins, F. Fu, and K. Gao. 2017. Effects of ultraviolet radiation on photosynthetic performance and N<sub>2</sub> fixation in *Trichodesmium erythraeum* IMS101. *Biogeosciences* **14**: 4455–4466.
- Capone, D. G. 1993. Determination of nitrogenase activity in aquatic samples using the acetylene reduction procedure, p. 621–631. *In* P. F. Kemp, B. F. Sherr, E. B. Sherr, and J. J. Cole [eds.], *Current methods in aquatic microbiology*. Lewis Publishers.
- Capone, D. G., J. P. Zehr, H. W. Paerl, B. Bergman, and E. J. Carpenter. 1997. *Trichodesmium*, a globally significant marine cyanobacterium. *Science* **276**: 1221–1229.
- Capone, D. G., and others. 2005. Nitrogen fixation by *Trichodesmium* spp.: An important source of new nitrogen to the tropical and subtropical North Atlantic Ocean. *Global Biogeochem. Cycl.* **19**: GB2024.
- Chen, Y.-B., J. P. Zehr, and M. Mellon. 1996. Growth and nitrogen fixation of the diazotrophic filamentous nonheterocystous cyanobacterium *Trichodesmium* sp. IMS 101 in defined media: Evidence for a circadian rhythm. *J. Phycol.* **32**: 916–923.
- Chen, Z., H.-B. Jiang, K. Gao, and B.-S. Qiu. 2020. Acclimation to low ultraviolet-B radiation increases photosystem I abundance and cyclic electron transfer with enhanced photosynthesis and growth in the cyanobacterium *Nostoc sphaeroides*. *Environ. Microbiol.* **22**: 183–197.
- Cullen, J. J., P. J. Neale, and M. P. Lesser. 1992. Biological weighting function for the inhibition of phytoplankton photosynthesis by ultraviolet radiation. *Science* **258**: 646–650.
- Doney, S. C., D. S. Busch, S. R. Cooley, and K. J. Kroeker. 2020. The impacts of ocean acidification on marine ecosystems and reliant human communities. *Annu. Rev. Env. Resour.* **45**: 83–112.
- Dutkiewicz, S., and others. 2015. Impact of ocean acidification on the structure of future phytoplankton communities. *Nat. Clim. Change* **5**: 1002–1006.
- Gao, G., W. Liu, X. Zhao, and K. Gao. 2021. Ultraviolet radiation stimulates activity of CO<sub>2</sub> concentrating mechanisms in a bloom-forming diatom under reduced CO<sub>2</sub> availability. *Front. Microbiol.* **12**: 651567.
- Gao, K., E. W. Helbling, D. P. Häder, and D. A. Hutchins. 2012. Responses of marine primary producers to interactions between ocean acidification, solar radiation, and warming. *Mar. Ecol. Prog. Ser.* **470**: 167–189.
- Gao, K., Y. Wu, G. Li, H. Wu, V. E. Villafañe, and E. W. Helbling. 2007. Solar UV radiation drives CO<sub>2</sub> fixation in marine phytoplankton: A double-edged sword. *Plant Physiol.* **144**: 54–59.
- Gao, K., G. Gao, Y. Wang, and S. Dupont. 2020. Impacts of ocean acidification under multiple stressors on typical organisms and ecological processes. *Mar. Life Sci. Technol.* **2**: 279–291.
- Gao, K., W. Zhao, and J. Beardall. 2022. Future responses of marine primary producers to environmental changes. *In* S. C. Maberly and B. Gontero [eds.], *Blue planet, red and green photosynthesis: Productivity and carbon cycling in aquatic ecosystems*. Wiley-ISTE.
- Gao, Q., and F. Garcia-Pichel. 2011. Microbial ultraviolet sunscreens. *Nat. Rev. Microbiol.* **9**: 791–802.
- Garcia, N. S., and others. 2011. Interactive effects of irradiance and CO<sub>2</sub> on CO<sub>2</sub> fixation and N<sub>2</sub> fixation in the diazotroph *Trichodesmium erythraeum* (cyanobacteria). *J. Phycol.* **47**: 1292–1303.
- Goebel, N. L., C. A. Edwards, B. J. Carter, K. M. Achilles, and J. P. Zehr. 2008. Growth and carbon content of three different-sized diazotrophic cyanobacteria observed in the subtropical north Pacific. *J. Phycol.* **44**: 1212–1220.
- Häder, D.-P., and others. 2015. Effects of UV radiation on aquatic ecosystems and interactions with other environmental factors. *Photochem. Photobiol. Sci.* **14**: 108–126.
- Hakala, M., I. Tuominen, M. Keränen, T. Tyystjärvi, and E. Tyystjärvi. 2005. Evidence for the role of the oxygen-evolving manganese complex in photoinhibition of photosystem II. *Biochim. Biophys. Acta Bioenerg.* **1706**: 68–80.
- Hong, H., and others. 2017. The complex effects of ocean acidification on the prominent N<sub>2</sub> fixing cyanobacterium *Trichodesmium*. *Science* **356**: 527–531.
- Hutchins, D. A., and others. 2007. CO<sub>2</sub> control of *Trichodesmium* N<sub>2</sub> fixation, photosynthesis, growth rates, and elemental ratios: Implications for past, present, and future ocean biogeochemistry. *Limnol. Oceanogr.* **52**: 1293–1304.
- Hutchins, D. A., M. R. Mulholland, and F. Fu. 2009. Nutrient cycles and marine microbes in a CO<sub>2</sub>-enriched ocean. *Oceanography* **22**: 128–145.
- Hutchins, D. A., F. Fu, N. G. Walworth, M. D. Lee, M. A. Saito, and E. A. Webb. 2017. Comment on “The complex effects of ocean acidification on the prominent N<sub>2</sub>-fixing cyanobacterium *Trichodesmium*”. *Science* **357**: eaao0067.
- Kana, T. M. 1993. Rapid oxygen cycling in *Trichodesmium thiebautii*. *Limnol. Oceanogr.* **38**: 18–24.
- Kranz, S. A., O. Levitan, K.-U. Richter, O. Prášil, I. Berman-Frank, and B. Rost. 2010. Combined effects of CO<sub>2</sub> and light on the N<sub>2</sub>-fixing cyanobacterium *Trichodesmium* ims101: Physiological responses. *Plant Physiol.* **154**: 334–345.
- Kumar, A., M. B. Tyagi, P. N. Jha, G. Srinivas, and A. Singh. 2003. Inactivation of cyanobacterial nitrogenase after exposure to ultraviolet-B radiation. *Curr. Microbiol.* **46**: 380–384.
- LaRoche, J., and E. Breitbart. 2005. Importance of the diazotrophs as a source of new nitrogen in the ocean. *J. Sea Res.* **53**: 67–91.
- Levitan, O., and others. 2007. Elevated CO<sub>2</sub> enhances nitrogen fixation and growth in the marine cyanobacterium *Trichodesmium*. *Glob. Chang. Biol.* **13**: 531–538.

- Luo, Y. W., I. D. Lima, D. M. Karl, C. A. Deutsch, and S. C. Doney. 2014. Data-based assessment of environmental controls on global marine nitrogen fixation. *Biogeosciences* **11**: 691–708.
- Luo, Y.-W., and others. 2019. Reduced nitrogenase efficiency dominates response of the globally important nitrogen fixer *Trichodesmium* to ocean acidification. *Nat. Commun.* **10**: 1521.
- Milligan, A. J., I. Berman-Frank, Y. Gerchman, G. C. Dismukes, and P. G. Falkowski. 2007. Light-dependent oxygen consumption in nitrogen-fixing cyanobacteria plays a key role in nitrogenase protection. *J. Phycol.* **43**: 845–852.
- Mulholland, M. R., P. W. Bernhardt, C. A. Heil, D. A. Bronk, and J. M. O'Neil. 2006. Nitrogen fixation and release of fixed nitrogen by *Trichodesmium* spp. in the Gulf of Mexico. *Limnol. Oceanogr.* **51**: 1762–1776.
- Neale, P. J., and B. C. Thomas. 2017. Inhibition by ultraviolet and photosynthetically available radiation lowers model estimates of depth-integrated picophytoplankton photosynthesis: Global predictions for *Prochlorococcus* and *Synechococcus*. *Glob. Chang. Biol.* **23**: 293–306.
- Nishiyama, Y., S. I. Allakhverdiev, and N. Murata. 2006. A new paradigm for the action of reactive oxygen species in the photoinhibition of photosystem II. *Biochim. Biophys. Acta* **1757**: 742–749.
- Ohnishi, N., and others. 2005. Two-step mechanism of photo-damage to photosystem II: Step 1 occurs at the oxygen-evolving complex and step 2 occurs at the photochemical reaction center. *Biochemistry* **44**: 8494–8499.
- Pathak, J., H. Ahmed, Rajneesh, S. P. Singh, D.-P. Häder, and R. P. Sinha. 2019. Genetic regulation of scytonemin and mycosporine-like amino acids (MAAs) biosynthesis in cyanobacteria. *Plant Gene* **17**: 100172.
- Piazena, H., E. Perez-Rodrigues, D. P. Häder, and F. Lopez-Figueroa. 2002. Penetration of solar radiation into the water column of the central subtropical Atlantic Ocean—Optical properties and possible biological consequences. *Deep-Sea Res. II Top. Stud. Oceanogr.* **49**: 3513–3528.
- Pinheiro, J. C., and D. M. Bates. 2006. *Mixed-effects models in S and S-PLUS*. Springer.
- Prufert-Bebout, L., H. W. Paerl, and C. Lassen. 1993. Growth, nitrogen fixation, and spectral attenuation in cultivated *Trichodesmium* species. *Appl. Environ. Microbiol.* **59**: 1367–1375.
- Rath, J., and S. P. Adhikary. 2007. Response of the estuarine cyanobacterium *Lyngbya aestuarii* to UV-B radiation. *J. Appl. Phycol.* **19**: 529–536.
- Rastogi, R. P., Richa, A. Kumar, M. B. Tyagi, and R. P. Sinha. 2010a. Molecular mechanisms of ultraviolet radiation-induced DNA damage and repair. *J. Nucl. Acids* **2010**: 592980.
- Rastogi, R. P., S. P. Singh, D.-P. Häder, and R. P. Sinha. 2010b. Detection of reactive oxygen species (ROS) by the oxidant-sensing probe 2',7'-dichlorodihydrofluorescein diacetate in the cyanobacterium *Anabaena variabilis* PCC 7937. *Biochem. Biophys. Res. Commun.* **397**: 603–607.
- Rastogi, R. P., and others. 2014. Ultraviolet radiation and cyanobacteria. *J. Photochem. Photobiol. B Biol.* **141**: 154–169.
- Raven, J. A. 2011. The cost of photoinhibition. *Physiol. Plant.* **142**: 87–104.
- Raven, J. A., J. Beardall, and A. Quigg. 2020. Light-driven oxygen consumption in the water-water cycles and photorespiration, and light stimulated mitochondrial respiration, p. 161–178. *In* A. W. D. Larkum, A. R. Grossman, and J. A. Raven [eds.], *Photosynthesis in algae: Biochemical and physiological mechanisms*. Springer International Publishing.
- Ritchie, R. J. 2006. Consistent sets of spectrophotometric chlorophyll equations for acetone, methanol and ethanol solvents. *Photosynth. Res.* **89**: 27–41.
- Rodriguez, I. B., and T.-Y. Ho. 2014. Diel nitrogen fixation pattern of *Trichodesmium*: The interactive control of light and Ni. *Sci. Rep.* **4**: 4445.
- Rouco, M., S. T. Haley, H. Alexander, S. T. Wilson, D. M. Karl, and S. T. Dyhrman. 2016. Variable depth distribution of *Trichodesmium* clades in the North Pacific Ocean. *Env. Microbiol. Rep.* **8**: 1058–1066.
- Shang, J.-L., and others. 2018. UV-B induced biosynthesis of a novel sunscreen compound in solar radiation and desiccation tolerant cyanobacteria. *Environ. Microbiol.* **20**: 200–213.
- Shi, D., S. A. Kranz, J.-M. Kim, and F. M. M. Morel. 2012. Ocean acidification slows nitrogen fixation and growth in the dominant diazotroph *Trichodesmium* under low-iron conditions. *Proc. Natl. Acad. Sci.* **109**: E3094–E3100.
- Shi, D., R. Shen, S. A. Kranz, F. M. M. Morel, and H. Hong. 2017. Response to comment on “The complex effects of ocean acidification on the prominent N<sub>2</sub>-fixing cyanobacterium *Trichodesmium*”. *Science* **357**: ea0428.
- Stocker, T. F., and others [eds.]. 2013. IPCC, 2013: Climate change 2013: The physical science basis. *In* Contribution of Working Group I to the Fifth Assessment Report of the Intergovernmental Panel on Climate Change. Cambridge Univ. Press.
- Tang, W., and N. Cassar. 2019. Data-driven modeling of the distribution of diazotrophs in the global ocean. *Geophys. Res. Lett.* **46**: 12258–12269.
- Tedetti, M., and R. Sempéré. 2006. Penetration of ultraviolet radiation in the marine environment: A review. *Photochem. Photobiol.* **82**: 389–397.
- Tedetti, M., and others. 2007. High penetration of ultraviolet radiation in the south east Pacific waters. *Geophys. Res. Lett.* **34**: L12610.
- Westberry, T. K., and D. A. Siegel. 2006. Spatial and temporal distribution of *Trichodesmium* blooms in the world's oceans. *Global Biogeochem. Cycl.* **20**: GB4016.
- Wood, S. N. 2017. *Generalized additive models: An introduction with R*, 2nd ed. Chapman and Hall/CRC.
- Wu, H., K. Gao, Z. Ma, and T. Watanabe. 2005a. Effects of solar ultraviolet radiation on biomass production and

- pigment contents of *Spirulina platensis* in commercial operations under sunny and cloudy weather conditions. *Fish. Sci.* **71**: 454–456.
- Wu, H., K. Gao, V. E. Villafañe, T. Watanabe, and E. W. Helbling. 2005b. Effects of solar UV radiation on morphology and photosynthesis of filamentous cyanobacterium *Arthrospira platensis*. *Appl. Environ. Microbiol.* **71**: 5004–5013.
- Yi, X., F. X. Fu, D. A. Hutchins, and K. Gao. 2020. Light availability modulates the effects of warming in a marine N<sub>2</sub> fixer. *Biogeosciences* **17**: 1169–1180.
- Zehr, J. P. 2011. Nitrogen fixation by marine cyanobacteria. *Trends Microbiol.* **19**: 162–173.
- Zehr, J. P., and D. G. Capone. 2020. Changing perspectives in marine nitrogen fixation. *Science* **368**: eaay9514.
- Zhu, Z., and others. 2020. Interactions between ultraviolet radiation exposure and phosphorus limitation in the marine nitrogen-fixing cyanobacteria *Trichodesmium* and *Crocospaera*. *Limnol. Oceanogr.* **65**: 363–376.
- Zuur, A. F., E. N. Ieno, N. J. Walker, A. A. Saveliev, and G. M. Smith. 2009. Mixed effects models and extensions in ecology with R. Springer.

### Acknowledgments

The study was supported by National Natural Science Foundation of China (41721005, 41890803, 41720104005). The authors are grateful to Professor John Beardall for his editorial help on the manuscript and to the laboratory engineers Xianglan Zeng and Wenyan Zhao for their logistical and technical support.

### Conflict of Interest

None declared.

Submitted 21 June 2022

Revised 19 September 2022

Accepted 15 December 2022

Deputy editor: C. Elisa Schaum